Long-Legged Hexapod Giacometti Robot Using Thin Soft McKibben Actuator

Ahmad Athif Mohd Faudzi, *Member, IEEE*, Gen Endo, *Member, IEEE*, Shunichi Kurumaya, and Koichi Suzumori, *Member, IEEE*

***Abstract*—This letter introduces a lightweight hexapod robot, Giacometti robot, made with long and narrow legs following the Alberto Giacometti's sculpture conception. The goal is achieved by, first, using multiple links with thin and soft McKibben actuators, and second, choosing a leg design which is narrow in comparison to its body's length and height, unlike conventional robot design. By such design characteristic, the leg will exhibit elastic deformations due to the low stiffness property of the thin link structure. Then, we model the leg structure and conduct the deflection analysis to confirm the capability of the leg to perform walking motion. The high force to weight ratio characteristics of the actuator provided the ability to drive the system, as shown by a static model and further validated experimentally. To compensate for the high elastic structural flexibility of the legs, two walking gaits namely customized Wave gait and Giacometti gait were introduced. The robot could walk successfully with both gaits at maximum speed of 0.005 and 0.05 m/s, respectively. It is envisaged that the lightweight Giacometti robot design can be very useful in legged robotic exploration.**

***Index Terms*—Giacometti structure, hexapod robot, legged locomotion, McKibben actuator, soft actuator.**

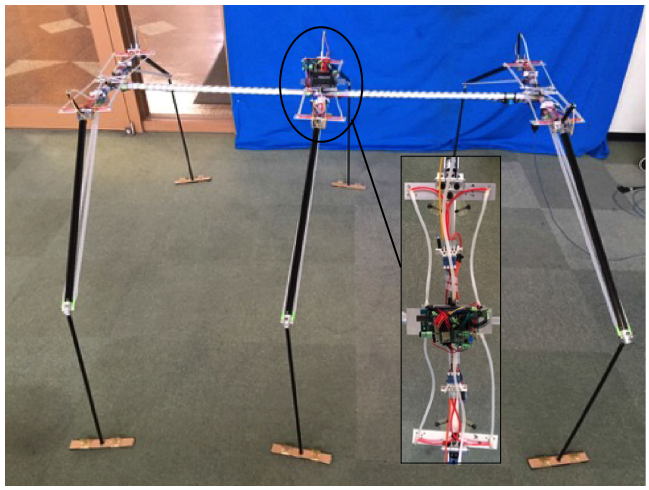

Fig. 1. The Giacometti robot and its control system.

I. Introduction

SINCE the time they introduced robots, researchers have developed robot's performance with various sensory equipment in order to resolve many applied problems [1]–[6]. Although highly functional robots with qualified specification have been proposed, they have complicated control systems and heavy bodies. This causes technical problems related to safety in practical. For example, if a robot falls or hits something beyond its control, the damage to the robot and the surrounding would be very large.

We have proposed a new concept robotics namely Giacometti robotics, which has the potential to solve these problems as the design is very different from conventional robots [7]. This concept is inspired by the work of Alberto Giacometti, a Swiss sculpture who most of his artistic style of essential design is to remove flesh of the subject. Fig. 1 shows the proposed Hexapod Giacometti robot which aims for a large body structure with long legs but having lightweight and simple system for observation purpose with minimal payload. Giacometti robotics aims to realize robots that are very light and simple, easy to handle, and essentially safe by emphasis on an essential function and less focus on the other functions. Other Giacometti robots includes 7 m-long Giacometti Arm, which uses helium-filled inflatable balloons that compensate for self-weight particularly developed in the feasibility of inspection [8]. From this design objective, our robot tries to reduce the weight of the robot by using soft and thin McKibben actuators and design small diameter leg size in comparison to its body's length and height, which differs from the conventional robot design.

Conventional design issues and principles for legged robots were presented by [6] where mechanical structure, leg design configuration, driving system and walking gait are among design procedures to consider. The Square-Cube Law [9] by Galileo (1564–1642) gives insight to the legged robot designer to decide the structural design [10]. From biomechanics point of view, the law mentioned that if allometric scaling were applied to an animal structure, its relative muscular strength would be severely reduced, since the cross section of its muscles would increase by the square of the scaling factor while its mass would increase by the cube of the scaling factor [11]. From this, robot designers understood that for bigger legged robots, the internal

Manuscript received February 15, 2017; accepted June 20, 2017. Date of publication July 31, 2017; date of current version August 17, 2017. This letter was recommended for publication by Associate Editor C. Laschi and Editor Y. Sun upon evaluation of the reviewers' comments. This work was supported by the JSPS KAKENHI under Grant 15K13907. *(Corresponding author: Ahmad Athif Mohd Faudzi.)*

A. A. M. Faudzi is with the Faculty of Electrical Engineering, Universiti Teknologi Malaysia, Johor Bahru 81310, Malaysia, with the Centre for Artificial Intelligence and Robotics, Universiti Teknologi Malaysia International Campus, Kuala Lumpur 54100, Malaysia, and also with the Department of Mechanical Engineering, Tokyo Institute of Technology, Tokyo 152-8552, Japan (e-mail: athif@utm.my).

G. Endo, S. Kurumaya, and K. Suzumori are with the Department of Mechanical Engineering, Tokyo Institute of Technology, Tokyo 152-8552, Japan (e-mail: gendo@mes.titech.ac.jp; kurumaya.s.aa@m.titech.ac.jp; suzumori.k.aa@m.titech.ac.jp).

Digital Object Identifier 10.1109/LRA.2017.2734244

stresses grow linearly with scale and therefore the elements of the structures must be thick in proportion to the strength thus bigger diameter and rigid legs should be designed. Big robots like Ambler with 2500 kg [4] and ATHLETE with 850 kg [5], have bigger structure and bigger leg diameter to support the body, as they must carry proportionately higher weight. These robots may have advantage to negotiate larger steps and may be more suitable for specific applications planetary exploration by Ambler and ATHLETE. Recently Ant-Roach, hexapod robot having big structure and big leg diameter but having overall weight of only 32 kg was reported. It applies inflatable structures using polybag material controlled with pressurized air to make the leg stiff [12]. On the other hand, thin legs architecture with small diameter was also proposed for legged robot. Hexapod Lunar rover from Institute of Automatics, Rome has straight leg with 2 DOF for each leg [13]. It consists of a hinge type rotary joint on its lateral axis and manipulates leg length by telescopic sliding structure at the knee joint making motion of the leg like that of an articulated leg. The design can reduce the shear stress for the leg and increase its rigidity.

Looking at the biological approach, a thin-legged insect which possesses non-proportional leg to body size like the Giacometti robot is the *Opiliones*, the animal commonly known as "harvestman" [14]. Harvestman is known for its long and thin structure where the legs will have special characteristics of elastic deformation from its low stiffness leg structure as one of its attractive features. Previous work of R. Hodoshima and S. Hirose proposed ASURA I [15] and KUMO-I [16] respectively which imitate the harvestman by having long slender rigid legs relative to its body. Although the study proves that it is possible for smaller diameter of leg size to drive a bigger structure robot, it has limited motion and suffers from poor back drivability due to its weight.

Therefore, Giacometti robot proposes to use lightweight structure from the thin soft McKibben actuator as its driving elements in antagonistic pairs and applies thin leg structure. The conventional McKibben muscle is bulky thus increases the overall weight of other pneumatically driven robots such as Pneupard [17] and AirBug [18]. As part of the Giacometti concept of simplicity, the first stage evaluation does not apply any sensor feedback reading unlike normal legged robots. The robot will fully rely on its mechanical body and leg structure using simple control loop without much dependence on the main brain. A customized gait, namely Giacometti gait is specially designed and proposed for the walking test. This concept shows that there is an exception with the above Galileo Square-Cube Law as the leg diameter used in the design is relatively small.

The current study contributes to our knowledge by addressing two issues; 1) new long-legged design concept, a shift in paradigm from the Square-Cube Law with static analysis of leg model, 2) new walking gait with simple control system. The remainder of the letter is organized as follows. In Section II, the soft thin actuator characteristics are explained. The force and contraction ratio data of 4.0 mm actuator is presented. Section III discusses robot design structure with the leg mechanism and its static stress and curve analysis. Section IV explains the system setup and discusses the customized Wave and Giacometti gait. The robot basic walking experiment using both gaits and other experiments are discussed in Section V. Finally, the letter concludes with a brief appraisal and future recommendation in Section VI.

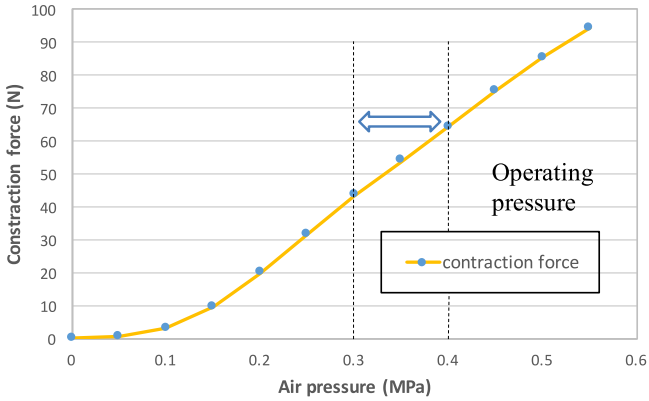

Fig. 2. Contraction ratio (%) and contraction force at different input pressure (MPa).

II. Thin Soft McKibben Actuator

A. Actuator Characteristics

Soft actuators are presently gaining popularity in many robots because of the advantages of high power-to-weight ratio, high compliance, flexible structure, strong reliability for human use and low cost for manufacturing the actuators [19]. McKibben actuator can generate high linearity in force [20] with low hysteresis and dead zone at low pressure. Smaller diameter of McKibben actuator had been developed with many different application [21]. We developed thin soft McKibben muscles for mass production [22]. The muscles are light, small, and suitable for simple systems [23]. The Giacometti robot applies 4.0 mm McKibben actuators which will contract when being pressurized with air. During contraction, the stiffness increases and produces contraction force providing the robot motion. The 4.0 mm silicone rubber tube is covered by 48 fibers of 0.22 mm Tetron monofilament and braided with 18 degrees for optimum contraction function of the actuator. Therefore, the overall outer diameter of the actuator is 4.6 mm.

B. Force Characterization

The static characteristics of the McKibben muscles were experimentally obtained by changing the input pressure. The actuators exhibit a contraction force proportional with the contraction ratio. This is confirmed with force characterization experiments reported [24]. Fig. 2 shows the characteristics of the 4.0 mm actuator when pressurized from 0 MPa to 0.6 MPa. The static characteristics were investigated by measuring the relationship between the generated force and contraction ratio under various pressure levels. The proposed operating pressure for the Giacometti robot is between 0.3 to 0.4 MPa. The contraction ratio of thin McKibben actuator is like some vertebrae muscle, which usually shortens by 25% or less [25]. The maximum force of the actuator at 0.3 MPa and 0.4 MPa is around 43 N and 65 N, respectively. Based on the contraction ratio and force of the actuator, the leg mechanism design of the Hexapod Giacometti is performed and will be describe in next section.

III. Leg Mechanism and Robot Structure

Insects normally have four main segments of coxa, femur, tibia and tarsus. Most of the length of insect leg is contributed by two long and nearly equally segments of femur and tibia.

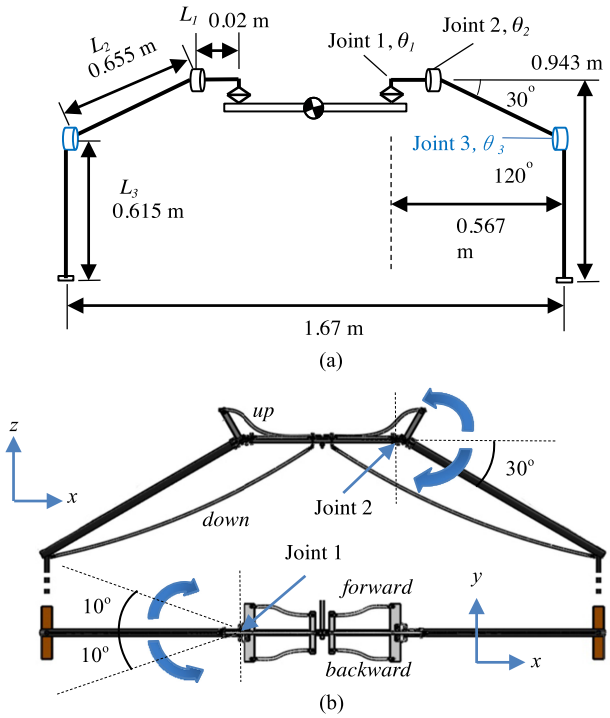

Fig. 3. Schematic diagram (a) and CAD design (b) of the robot structure.

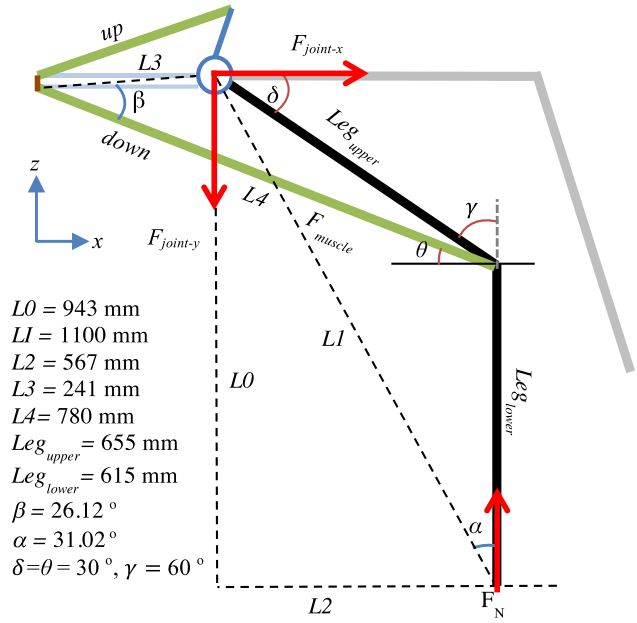

Fig. 4. Single leg model of Giacometti robot.

However, for *Opiliones* [14], the tarsus length is longer making it has exceptionally long legs relative to their body size. The Giacometti robot is proposed to have long legs to be more adaptive to ground unevenness. Having longer legs is also an advantage managing larger steps compared to shorter legged robots. The hexapod Giacometti simplifies the design by reducing the number of actuated joints on each leg to two degrees of freedom (DoF) with making the total amount of DoF to 12. With the reduced actuated joints, the robot is expected to maintain its ability of body propulsion in the horizontal plane and its transition between the swinging phase and the stance phase. The six legs were distributed symmetrically along two sides of the body structure, each having three legs. It was described the leg placement to be more stable in longitudinal margin compared to hexagonal architecture [6]. Practicable walking gaits were tested and investigated using this architecture [1].

A. Leg Model and Structure

The leg is modeled as shown in schematic diagram and CAD design as in Fig. 3. Each leg has two DoF of yaw and roll motion using two hinge joints. The hinge Joint 1, θ_1 and Joint 2, θ_2 is the yaw joint and roll joint respectively. Joint 1 is the hip joint that rotates parallel to the ground around vertical axis while Joint 2 is a revolute joint around horizontal axis. For yaw motion, the leg can move forward and backward while for roll motion, the leg can be raised up and down. The leg parts relate to equally segments of femur, Leg_{upper} and tibia Leg_{lower}. The knee joint was fixed at an imaginary Joint 3, 120° from *L3* to simplify the leg design, and limit the roll motions only Joint 2. The yaw on Joint 1 has range of motion from $-10°$ to 10° while Joint 2 has range of motion from 0° to 30°. For both Joint 1 and Joint 2, two actuators are placed at each joint and work as an agonist–antagonist pair of muscles; when one-muscle contracts, the other relaxes. Looking at the biological aspect, synergistic of the muscle system would contribute to the isometric function like human bicep and triceps as well as leg muscles for terrestrial animals [17]. Fig. 4 shows the analysis of one leg of Giacometti robot. Green line represents the antagonistic muscles of *up* and *down* at Joint 2.

The Giacometti robot has 0.943 m height, 1.67 m width, 1.5 m length and 3.7 kg weight (without air compressor). The diameter of the upper leg is 20 mm, and for the lower leg it is only 10 mm. The leg diameter is selected to mimick the leg property of Opiliones that exhibit elastic deformation from the long and thin leg structure and follow the concept of Giacometti. However, thin legs have higher potential to break due to the overall body weight. Longer beams such as long bones of a vertebrae limb are more likely to experience large bending-induced stresses than short links [26]. Therefore, we lessen the weight of the robot structure by using aluminum and selected CFRP pipe to be used as the leg links, which is known for its lightweight and toughness to support possible bending from the system. Static stress analysis was performed for the robot design by deflection measurements to confirm the capability of the leg links, Leg_{upper} and Leg_{lower}, as in the Sections B and C. The hinge and stopper design were fabricated using a 3D printer with ABS material. The leg can rise to 320 mm and have stride, λ of 400 mm from the 20° angle. No mechanism was added for the foot as the mass at the end of the leg largely affects the inertia of the leg. A 160 mm $\times$ 30 mm wood was only attached at the sole to increase friction coefficient and the improve the stability to support the robot during walking motion.

B. Model of Static Stress Analysis

Carbon fiber reinforced polymer (CFRP) is used as the leg material for the robot where it provides lightweight and strength to the structure as in Fig. 4. To analyze the stress in the legs, two segments were considered, Leg_{upper} *and* Leg_{lower}. The boundary condition is assumed to be free movement while at the other end, it is regarded as fixed. Given the inner diameter (D_i)

TABLE I
SECTION PROPERTIES OF CFRP

Leg part	Diameter ($D_o \times D_i$)	Cross-sectional area (A_{CFRP})	Section modulus (Z_{CFRP})	Max Stress $\sigma\sigma_{m1}$	Max Stress σ_{m2}
Leg_{upper}	(20 × 19) mm	31 mm^2	146 mm^3	1.018 MPa	2.188 MPa
Leg_{lower}	(10 × 9) mm	15 mm^2	34 mm^3	3.08 MPa	4.771 MPa

and outer diameter (D_o), its cross-sectional area, A_{CFRP} and section modulus, Z_{CFRP} along the neutral axis can be calculated as follows

$$A_{\text{CFRP}} = \frac{\pi(D_0^2 - D_i^2)}{4} \tag{1}$$

$$Z_{\text{CFRP}} = \frac{\pi(D_o^4 - D_i^4)}{32D_o} \tag{2}$$

Note that the critical stresses acting at Leg_{lower} and Leg_{upper} are going to be studied for selection of proper leg diameter with appropriate strength. The maximum stress, σ_m in hollow pipes is the sum of normal stress resulting from compression, σ_c and bending, σ_b. Therefore, in Leg_{lower} the stress can e calculated as follows

$$\sigma_{m1} = \sigma_{c1} + \sigma_{b1} \tag{3}$$

$$\sigma_{c1} = \frac{F_{\text{muscle}}\sin\beta - F_N}{A_{\text{CFRP}}}, \sigma_{b1} = \frac{F_{\text{muscle}}\cos\beta}{Z_{\text{CFRP}}} \tag{4}$$

Similarly, in Leg_{upper} stress can be calculated as follows

$$\sigma_{m2} = \sigma_{c2} + \sigma_{b2} \tag{5}$$

$$\sigma_{c1} = \frac{F_{joint-x}\sin\gamma + F_{joint-y}\cos\gamma}{A_{\text{CFRP}}} \tag{6a}$$

$$\sigma_{b2} = \frac{F_{joint-x}\cos\gamma - F_{joint-y}\sin\gamma}{Z_{\text{CFRP}}} \tag{6b}$$

The selected CFRP material is a resin based carbon fiber material with tensile strength of 1860 MPa. For proper design, we included a factor of safety, *FS*, which is the stress when the material is deemed to fail. *FS* of 5 was considered, based on the walking experiment of the robot to be tested in robust environment including a fall test, where acting force is unpredictable and the magnitude or direction of force is uncertain thus the strength of the material is 372 MPa. Table I shows the calculated section properties and stress of the CFRP materials using (1)–(6). As all values are less than 372 MPa, which is safe for the design, 20 mm was selected as the outer diameter of Leg_{upper} and 10 mm as outer diameter of Leg_{lower}.

C. Deflection Curve Analysis

A load on a body that produces changes in the geometry of the body are known as deformation or compliant displacements [27]. Deflection curve analysis were performed to measure the stiffness which is the capacity of the leg structure to sustain load without excessive changes of its geometry. The legs are considered as nonprismatic cantilever beams as the Leg_{upper} and Leg_{lower} have different outer diameter of 20 mm and 10 mm, respectively, with fixed joint, 120° angle, as shown in Fig. 3. To simplify the calculation, it is assumed that both legs as single part with homogeneous hollow core structure. The beam-like elements with hollow core provide better resistance to bending for a given weight rather than solid cross sections while giving structural safety. Considering the applied force, *F*, modulus of elasticity, *E* of CFRP is 150 × 10^9 Pa and the moment of inertia, *I* given by

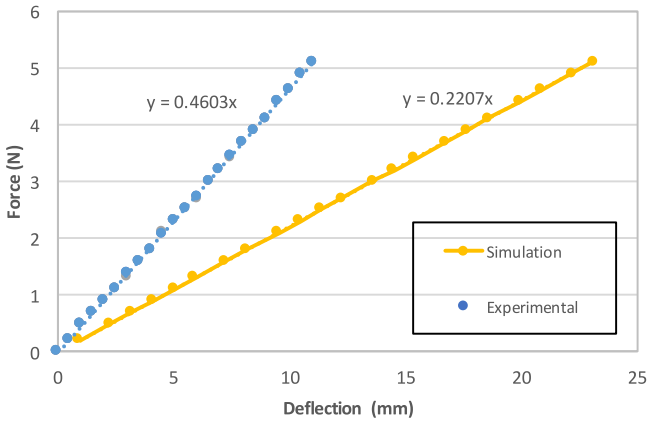

Fig. 5. Deflection curve experiment and theoretical comparison.

$$I = \frac{\pi}{64}(D_o^4 - D_i^4) \tag{7}$$

The deflection curve can be obtained for Leg_{lower}, $\delta_{Leg_{\text{lower}}}$

$$\delta_{Leg_{\text{lower}}} = \frac{F(Leg_{\text{lower}})^3}{3E(I_{Leg_{\text{lower}}})} \tag{8}$$

and for the Leg_{upper} deflection curve, $\delta_{Leg_{\text{upper}}}$

$$\delta_{Joint} = \frac{F(Leg_{\text{upper}})^3}{3E(I_{Leg_{\text{upper}}})} + \frac{(F \cdot Leg_{\text{upper}})(Leg_{\text{upper}})^2}{2E(I_{Leg_{\text{upper}}})} \tag{9}$$

$$\theta_{Joint} = \frac{F(Leg_{\text{upper}})^2}{2E(I_{Leg_{\text{upper}}})} + \frac{F(Leg_{\text{upper}})}{E(I_{Leg_{\text{upper}}})} \tag{10}$$

$$\delta_{Leg_{\text{upper}}} = \delta_{Joint} + \theta_{Joint} \cdot \left(\frac{Leg_{\text{upper}}}{2}\right) \tag{11}$$

$$\delta_{\text{total}} = \delta_{Leg_{\text{lower}}} + \delta_{Leg_{\text{upper}}} \tag{12}$$

The total deflection curve as in (12) is plotted in Fig. 5 and compared with the experimental results of the deflection curve test. The leg tip is connected to a force gauge and pulled using a DC motor on a linear guide. The experiment result shows the actual system is two times stiffer compared to the calculated deflection. A possible reason may due to the experimental setup and from the non-homogenous diameter of the leg parts of the CFRP pipe. Mismatch between theoretical and experimental result would require the development of more accurate stiffness model to improve the stiffness analysis [27].

The experiment shows the elastic property of the leg, which has the high non-stiffness property that could bend with displacement of 11 cm at 5 N. The Giacometti robot has unique leg structure and considers the leg deflection in its design objective.

D. Selection of Actuators Length

The actuators length for each part were decided based on actuator characteristics of contraction ratio and force as discussed in Section II. Based on the characteristics experiment of the actuator conducted in [24], it shows that the contraction ratio and force are the same at any length of the actuator. However, the contraction ratio changes at different pressure input e.g., 18.5% and 24% at 0.3 MPa and 0.35 MPa respectively.

The important aspect of the design is to ensure the robot can be supported with the contraction force of the muscles and possible to locomote. Each leg has two degrees of freedom (DoF) of roll and yaw, which requires 2 pairs of antagonistic muscles. First pair will perform roll motion of up and down, while the other pair executes yaw motion of forward and backward. The muscles were named based on its function of *up*, *down*, *forward* and *backward*. The pair of *up* and *down* muscles have different length however *forward* and *backward* muscles have the same length. The actuators length is important to know the muscles actuation capability to drive with the amount of force needed.

The robot structure is designed to allow the Giacometti robot to support as much payload as possible by choosing the correct actuator's length for stance position which applies the *down* muscles. From Fig. 4, the moment equilibrium around the *Joint 2* is presented by (13)

$$F_{\text{muscle}} = \frac{F_N(\sin\alpha \cdot L1)}{(\sin\beta \cdot L3)} \tag{13}$$

where F_{muscle} is the expected force required to support 1/3 of the whole payload of the system. Initially, it is considered that the robot will use minimum three legs for stance position. α is the angle during stance position perpendicular with the rotation point. β is the angle between the platform and the muscle. δ is the movements when the leg is raised up. Force exerted by the joint can obtain by (14) and (15).

$$F_{joint-y} = (F_{\text{muscle}} \cdot \sin\beta) - F_N = 18.01N \tag{14}$$

$$F_{joint-x} = (F_{\text{muscle}} \cdot \cos\beta) = 63.93N \tag{15}$$

The initial design specification of the Giacometti robot is expected to support overall weight and payload up to 4 kg (40 N) which requires each leg to support at least $F_N = 13.33$ N. By inserting F_N in (13), the required amount of F_{muscle} needed is 71.2 N. Based on the characteristics of the actuator in Fig. 2, the maximum contraction force at 0.3 MPa is only 43 N. Therefore, one link of actuator could not support the overall weight of the system. Adding more actuators in parallel [24] or increasing the operating pressure can be a solution to provide F_N.

Two links of the McKibben soft actuator that could support acting force, F_N of 86 N when operated at 0.3 MPa were added, thus supporting the $F_{\text{muscle}} = 71.2$ N. At 0.4 MPa, the actuator could support up to 130 N giving higher own weight to payload ratio. The *down* muscle's length, $x = 804$ mm is decided based on 3% of its contraction ratio from *L4* = 780 mm, which is the absolute displacement for stance to produce the amount of force needed using (16)

$$\frac{x - 780}{x} = 3\% \tag{16}$$

The length for *up* muscle was decided based on the 30° angle of the leg to be raised. The length is also decided based on the contraction ratio of the actuator. Finally, the length for yaw motion, *forward* and *backward* refers to the $+10°$ and $-10°$ and the actuator lengths are set accordingly. All four types of actuator are tabulated in Table II, which shows different length of muscles used.

TABLE II
SPECIFICATION OF ACTUATORS USED FOR GIACOMETTI ROBOT

Muscles	Leg function	Initial length	After pressurized
Down x (2)	Stance	804 mm	655 mm
Up	Swing	290 mm	235 mm
Forward	Forward	165 mm	135 mm
Backward	Backward	165 mm	135 mm

The robot uses 24 miniature on/off valves to control each actuator contraction. Each leg will have five actuators to be controlled using 4 on/off valves. Note that stance position requires two link of parallel actuator. With the distributed control applied, each muscle is pressure-controlled to follow the desired phase for walking motions.

IV. CONTROL SYSTEM AND WALKING GAIT

A. Control System and Walking Gait

The Giacometti robot is controlled using Arduino Mega 2560. The system is powered by two sets of 6 V DC Li-On batteries. DC-DC converter is used to convert to 24 V to drive the Koganei B005E1-PS on/off valves. The circuit is stacked together with the battery and placed at the center of the robot body to maintain the ZMP during the walking motion as in Fig. 1. Four valves are placed at each leg to reduce the air loss and provide faster air supply to the muscles. In the present design, the compressed air is supplied by an air compressor which is not on board, however on board installation of an air-tank is possible in the future.

Initial walking experiment was conducted using tripod gait. The whole-body structure can be supported with 3 legs during stance phase as calculated in Section III in static position like the Hexapedal creature e. g. Cockroach. However, due to the non-proportional length of the leg to the body and the elasticity characteristics of the leg that deflects, three legs in tripod gait could not achieve stable walking for Giacometti structure. The leg would bend and disturb the center of gravity making walking motion unstable to support during stance in dynamic motion. It is concluded that tripod gait is not suitable for this robot because of the leg deformation property. *Opiliones* on the other hand, could walk properly using tripod gait with it long legs because of its optimized God-created structure supported by 6-8 legs locomotion.

B. Customized Wave Gait

Customized Wave gait considers 5 legs to support the body during stance phase. It could adapt with the leg bending characteristics during the walking. The gait is designed so that, the vertical projection of center of gravity of the robot must be within the convex of the supporting polygon linked positions of all supporting feet which represent by the dotted line in Fig. 6. The gait is divided into seven phases and will be repeated for the walking motion. Phase 1 to phase 6 move each leg forward and phase 7 moves all the legs backward to achieve the robot's body forward motion. Fig. 6 shows the leg sequence and walking motion of the customized wave gait. The blue arrow shows

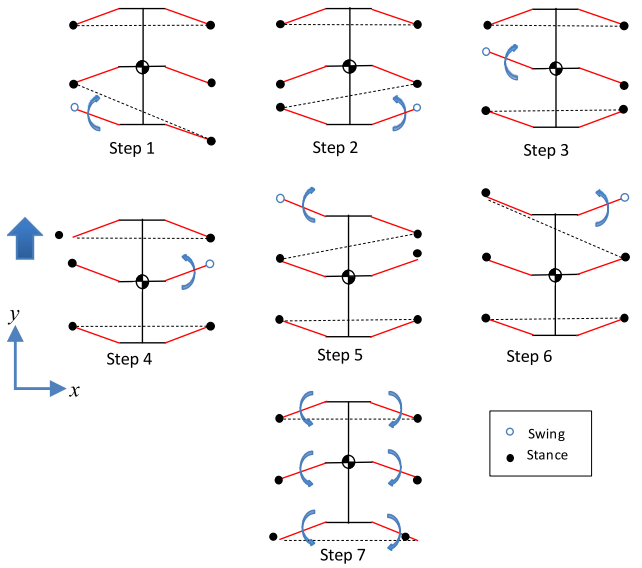

Fig. 6. Customized Wave gait walking pattern.

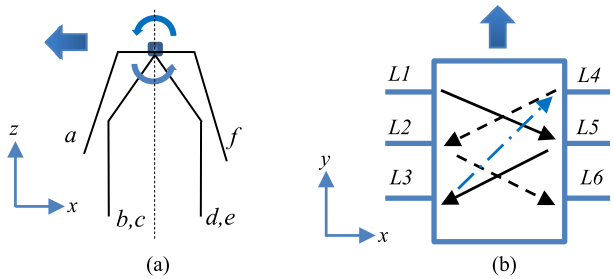

Fig. 7. Leg assignment for Giacometti gait (a) side view of one leg (b) top view.

the direction of robot motion. Five-leg support could achieve minimum requirement for the Giacometti robot walking motion. This gait could achieve stable motion from to the numbers of supported legs during stance phase however the speed of the gait is slow as 7-step gait of walking phase could achieve only one stride length, λ. The stride length of the gait is the distance by which the body of the robot is translated during complete step cycle.

C. Customized Giacometti Gait

Customized Giacometti gait is proposed to challenge the robot with minimum four legs during stance phase in walking motion. This gait also ensures the vertical projection of center of gravity of the robot is within the convex of the supporting polygon linked positions of all supporting feet. The gait is divided to six phases for walking motion. This gait is characterized by two condition in each step 1) two legs are in swing phase while the other four legs support the body structure in stance phase, 2) two legs are in motion while the other four legs maintain the position. Fig. 7(a) shows the leg assignment for the Giacometti gait from side view. *'a'* and *'f'* is the condition when the robot leg is in swing phase while *'b','c','d','e'* is condition during stance phase. The leg coordination of the Giacometti gait is shown in Fig. 7(b) following the order of arrows from *L1, L5, L3, L4, L2*

TABLE III
SPECIFICATION OF GIACOMETTI GAIT LEG ASSIGNMENT

Phase	L1	L5	L3	L4	L2	L6
Step 1	a	f	e	d	c	b
Step 2	b	a	f	e	d	c
Step 3	c	b	a	f	e	d
Step 4	d	c	b	a	f	e
Step 5	e	d	c	b	a	f
Step 6	F	e	d	c	b	a

a = swing forward *b*, *c* = stance forward.
d, *e* = stance backward *f* = swing backward.

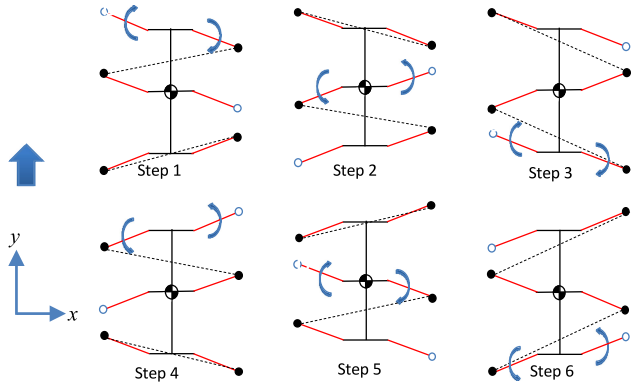

Fig. 8. Giacometti gait walking pattern.

and *L6*. The order will be continuously repeated for the forward motion. The leg assignment for each step will be decided based on condition from Table III. In step 1, *L1* will perform 'swing forward' while *L5* will perform 'swing backward' motion. Other flow of leg coordination as in Fig. 7(b) were tested, however the proposed arrangement above gives the best stability for the leg walking motion.

Fig. 8 shows the coordination of the walking phases and its leg sequence. In the first step of Step 1, *L2*, *L3*, *L4* and *L6* are in stance position while *L1* and *L5* are in swing phase. On the other hand, two legs are in motion, *L1* swings forward and *L4* performs a stance backward. The *L4*, which performs backward motion while in stance position, will produce forward body motion of the robot. However, as the other three legs are in contact with the ground in stance state, it prevents the robot body from performing any forward motion. This forces the *L4* to store the elastic energy developed towards the surface by bending its structure. This phenomenon is possible as the leg has bending structure capability from the low stiffness property. The stored elastic energy at the leg tip will be converted the kinetic energy, which pushes the robot for forward motion in the next phase. This unique gait makes it possible for the Giacometti robot to walk supported by four legs by applying the advantage of elastic and low stiffness leg structure. This 6-step gait will be repeated for the robot walking locomotion.

V. EXPERIMENTS AND DISCUSSION

A. Walking Test

Walking experiments were conducted for both customized Wave and Giacometti gaits. The challenge for the robot is to

Fig. 9. Walking motion sequence using Giacometti gait at interval of 2 seconds.

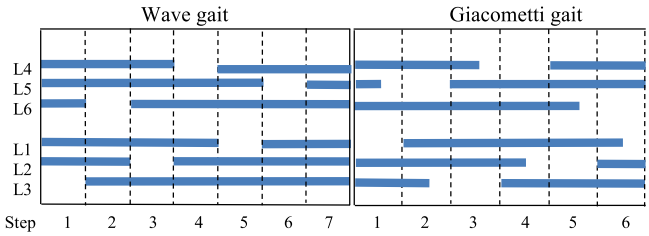

Fig. 10. Walking locomotion of wave gait and Giacometti gait.

walk with its low stiffness leg structure due to small diameter leg size. Basic walking test was conducted on even terrain for both gaits. Walking speed of Giacometti gait is 0.05 m/s while wave gait speed is 10 times slower with 0.005 m/s. This is because the wave gait requires 7 step to perform a single stride. Although the walking motion is slow compared to Giacometti gait, it gives maximum walking stability for Giacometti structure. On the other hand, Giacometti gait is designed in such way that it exploits structural flexibility of the legs. The Giacometti gait seems to be more practical with faster walking speed compared to wave gait. Fig. 9 shows walking motion sequence using Giacometti gait on terrain irregularities of up to 4 cm and compensate it by distributing the additional force with its elastic leg and its soft actuation system without additional sensors. Fig. 10 shows the locomotion of the wave gait and Giacometti gait for each step. The blue line represents the leg condition during stance phase during actual experiment. For Giacometti gait, it is noticed that there is a slight delay in leg lifting due to *up* and *down* antagonistic motion change. However, inversely this will give more support for the robot in stance phase.

B. Leg Bending Characteristics in Giacometti Gait

As discussed in Section IV-C, in each step of Giacometti gait, two legs are in motion and the other legs maintain the position. The moving legs on stance position convert their kinetic energy to elastic strain energy from the deformation of leg and release it back in the next phase as kinetic energy. The other 3 legs accommodate the bending of the active leg. Motion capture analysis was performed for single leg to observe the leg bending property as in Fig. 11. At t = 2.6 s and 11.3 s, the leg bends at 88° and 77°, respectively, from the surface ground. During lifting, the leg releases stored energy and this is confirmed by the increment of leg angle towards the surface. Due to the elastic effect, the leg exhibit small oscillation marked in red circle in Fig. 11. The stride of the leg was also confirmed, which is around 400 mm and the height of the tip at 320 mm during the walking experiment.

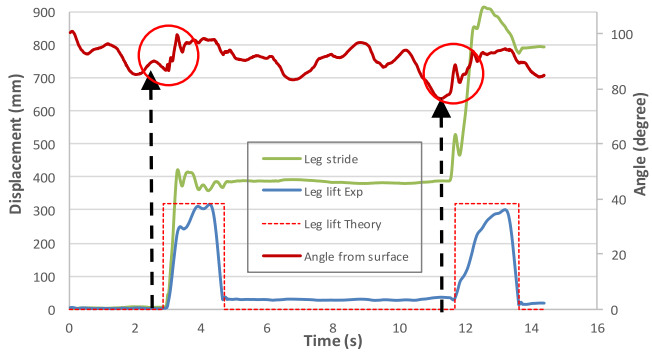

Fig. 11. Motion capture analysis of the leg during walking.

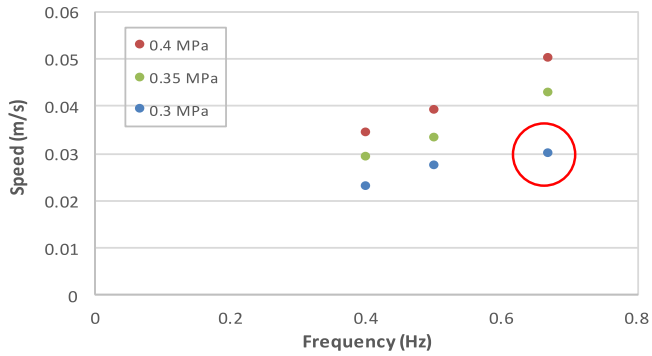

Fig. 12. Giacometti gait walking speed at different frequency and pressure input.

C. Frequency and Pressure

Further test was conducted for the Giacometti gait with different phase frequency and change the pressure input from 0.3 MPa to 0.4 MPa as in Fig. 12. The test is conducted only on the Giacometti gait as the Wave gait is relatively stable with it 5 legs during stance position. From the figure, it is understood that higher frequency can increase the walking speed. However, due to the soft actuator that requires time for contraction, too fast changes in each phase may result in unstable walking performance. The faster the muscle contracts, the less force it exerts until at the maximum possible rate of contraction, it exerts no force at all [25]. The marked circle in Fig. 12 shows the robot can walk for only a few steps and falls at 0.67 Hz and 0.3 MPa input pressure. On the other hand, higher input pressure in driving the actuator may help the actuator, providing more reliable walking motion. From this study, it is understood that the muscle can deliver its maximum possible power output only, if its rate of contraction is optimal for its physiological properties.

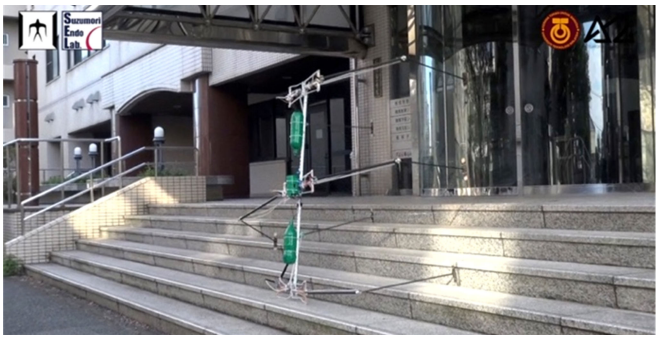

Fig. 13. Fall and recovery test (as in multimedia attachment).

D. Robustness Test

The robustness of the robot was assessed by performing fall and recovery experiment from 1 m height stairs as in Fig. 13. The test would result in serious damage for conventional robot; however, the damage to Giacometti robot and its surrounding was small. The robot is still able to perform basic walking after minimal recovery during the drop test. This shows the advantage of lightweight property of the robot and the structure.

VI. Conclusion

In this letter, a new "Giacometti" concept of robotics was proposed in which the leg structures are long, light and thin. Giacometti robot's leg mechanism and its model using 4.0 mm soft thin McKibben actuators were presented. The muscle lengths for stance, swing, forward and backward are based on robot design specification using the muscle's contraction ratio and contraction force characteristics. The prototype has successfully demonstrated basic walking using customized Wave gait and the Giacometti gait with minimum 4 legs to support its motion. This work indicated that although Giacometti robot structure exhibits elastic deformation due to small diameter leg size, the customized Giacometti gait utilizes this structural flexibility for a unique gait design for its walking capability on even and uneven surfaces. The walking gait was discussed with some parameter changes to see the effect of frequency and input pressure on the stability of walking motion. Finally, the robustness advantage of the robot was highlighted by allowing it to fall from 1 m height stairs. As an extension to the work, it would be interesting to conduct detail compliance analysis of the proposed structure and to study the dynamics of the leg elasticity with more complex control for optimized gait.

References

[1] X. Ding, Z. Wang, A. Rovetta, and J. M. Zhu, "Locomotion analysis of hexapod robot," in *Climbing and Walking Robots*. Rijeka, Croatia: InTech, 2010, p. 292.

[2] S. Kitano, "Study of mechanism and control of sprawling-type quadruped robot based on intermittent trot Gait," Ph.D. dissertation, Dept. Mech. Eng., Tokyo Inst. Technol., Tokyo, Japan, 2016.

[3] H. Komatsu, G. Endo, R. Hodoshima, S. Hirose and E. F. Fukushima, "How to optimize the slope walking motion by the quadruped walking robot," *Adv. Robot.*, vol. 29, no. 23, pp. 1497–1509, 2015.

[4] E. P. Krotkov, R. Simmons, W. L. Whittaker, "Ambler: Performance of a six-legged planatery rover," *Acta Astonautica*, vol. 35, no. 1, pp. 75–81, 1995.

[5] B. H. Wilcox *et al.*, "ATHLETE: A cargo handling and manipulation robot for the moon," *J. Field Robot.*, vol. 24, no. 5, pp. 421–434, 2007.

[6] F. Tedeschi and G. Carbone, "Design issues for hexapod walking robots," *J. Robot.*, vol. 3, pp. 181–206, 2014.

[7] K. Suzumori, "New pneumatic artificial muscle realizing Giacometti robotics and soft robotics," in *Proc. 6th Int. Conf. Manufact., Mach. Design Tribol.*, 2015, no. 15–204, pp. 4–5.

[8] M. Takeichi, K. Suzumori, G. Endo, and H. Nabae, "Development of Giacometti arm with balloon body," *IEEE Robot. Autom., Lett.*, vol. 2, no. 2, pp. 951–957, Apr. 2017.

[9] G. Galilei, *Discorsi e Dimostrazioni Matematiche Intorno a Due Nuove Scienze*. Amsterdam, Netherlands: Elsevier, 1638.

[10] S. Sakai, K. Osuka, and M. Umeda, "Global performance of agricultural robots," in *Proc. IEEE/RSJ Int. Conf. Intell. Robots Syst.*, 2004, pp. 461–466.

[11] S. M. Levin, "A different approach to the mechanics of the human pelvis: Tensegrity," *Movement, Stability and Low Back Pain*, A. Vleeming *et al.*, Eds. Edinburgh, U.K.: Churchill Livingstone, London, 1997.

[12] http://spectrum.ieee.org/automaton/robotics/diy/inflatable-antroach-robot-is-big-enough-to-ride

[13] U. Mocci, N. Petternella, and S. Salinari, "Experiments with six-legged walking machines with fixed gait," Inst. Autom., Rome Univ., Rome, Italy, Rep. 2-12, 1972.

[14] R. Pinto-da-Rocha, G. Machado, and G. Giribet, *HARVESTMAN: The Biology of Opiliones.*, Cambridge, MA, USA: Harvard Univ. Press, 2007.

[15] R. Hodoshima, S. Watanabe, Y. Nishiyama, A. Sakaki, Y. Ohura, and S. Kotosaka, "Development of ASURA I: harvestman-like hexapod walking robot—approach for Long-legged robot and leg mechanism design," in *Proc. IEEE/RSJ Int. Conf. Intell. Robot. Syst.*, 2013, pp. 4669–4674.

[16] S. Hirose and K. Kato, Study on quadruped walking robot in Tokyo institute of technology—past, present and future," in *Proc. IEEE Int. Conf. Robot. Autom.*, 2000, pp. 1–6.

[17] S. Nakatsu, A. Rosendo, M. Shimizu, and K. Hosoda, "Realization of three-dimensional walking of a cheetah-modeled bio-inspired quadruped robot," in *Proc. IEEE Int. Conf. Robot. Biomimetics*, 2014, pp. 779–784.

[18] T. Kerscher, J. Albiez, and K. Berns, "Joint control of the six-legged robot airbug driven by fluidic muscles," in *Proc. 3rd Int. Workshop Robot Motion Control*, 2002, pp. 27–32.

[19] I. N. A. M. Nordin, M. R. M. Razif, A. A. M. Faudzi, E. Natarajan, K. Iwata, and K. Suzumori, "3-D finite-element analysis of fiber-reinforced soft bending", in *Proc. IEEE/ASME Int. Conf. Adv. Intell. Mechatronics*, 2013, pp. 128–133.

[20] A. A. M. Faudzi, N. H. Izzuddin, and K. Suzumori, "Modeling and force control of thin soft McKibben actuator," *Int. J. Autom. Technol.*, vol. 10, no. 4, pp. 487–493, 2016.

[21] Y. K. Lee and I. Shimoyama, "A multi-channel micro valve for micro pneumatic artificial muscle," in *Proc. IEEE Int. Conf. Micro Electro Mech. Syst.*, 2002, pp. 702–705.

[22] M. Takaoka, K. Suzumori, S. Wakimoto, S. Iijima, and T. Tokumiya, "Fabrication of thin McKibben artificial muscle with various design parameters and their experimental evaluations," in *Proc. 5th Int. Conf. Manuf. Mach. Design Tribiol.*, 2013, pp. 82.

[23] A. A. M. Faudzi, M. R. M. Razif, G. Endo, H. Nabae, and K. Suzumori, "Soft-amphibious robot using thin and soft Mckibben actuator," in *Proc. IEEE Int. Conf. Adv. Intell. Mechatronics*, 2017, pp. 981–986.

[24] S. Kurumaya, K. Suzumori, H. Nabae, and S. Wakimoto, "Musculoskeletal lower-limb robot driven by multifilament muscles," *Robomech J.*, vol. 3, no. 18, pp. 1–15, 2016.

[25] R. McNeill Alexender, *Principles of Animal Locomotion*, Princeton, NJ, USA: Princeton Univ. Press, 2003.

[26] A. A. Biewener, *Animal Locomotion*. London, U.K.: Oxford Univ. Press, 2003.

[27] G. Carbone, "Stiffness analysis and experimental validation of robotic systems," *Frontiers Mech. Eng.*, vol. 6, no. 2, pp. 182–196, 2011.